Electrical and thermal tuning of quality factor and free spectral range of optical resonance of nematic liquid crystal microdroplets

Junaid Ahmad Sofi, M. A. Mohiddon, N. Dutta, and Surajit Dhara*
School of Physics, University of Hyderabad, Hyderabad 500046, India
(Received 22 March 2017; revised manuscript received 16 June 2017; published 4 August 2017)

We experimentally study the effect of temperature and electric field on the quality (Q) factor and free spectral range (FSR) of whispering-gallery-mode optical resonance of dye-doped nematic liquid crystal microdroplets. Both the Q factor and the FSR are highly sensitive to the temperature and electric field and are tunable. The Q factor decreases, whereas the FSR increases substantially, with increasing temperature and electric field. The variation of the Q factor and FSR is understood based on the change in the effective refractive index and the dynamic size of the microdroplets.

DOI: 10.1103/PhysRevE.96.022702

I. INTRODUCTION

Optical microcavities possess a small mode volume and high quality (Q) factor. These microresonators find wide application in laser sources, active filters, all-optical switches [1–4], etc. The high Q-factor value associated with the resonant modes make them highly sensitive biological and chemical sensors [5–13]. Their small size and easy tunability by external electric and magnetic fields make them future contenders as crucial components in photonic devices [14–17]. In spherical microcavities, the light circulates inside the sphere due to the total internal reflection provided the refractive index of the surrounding medium is lower than that of the microcavity. The resonance condition is achieved when the circulating light meets in-phase and this is known as whispering-gallery-mode (WGM) resonance. Solid dielectric-based spherical microresonators have a high quality factor and have been studied to a great extent [1]. However, they are not easily tunable by external fields such as electric and magnetic. In this context, liquid crystal (LC) based microresonators have drawn significant attention. Humar *et al.* first reported WGM resonance in nematic LC microdroplets [14]. Subsequently they showed three-dimensional lasing and surfactant sensing ability of the microdropets [15,16]. Wang *et al.* reported on the tunable WGM lasing of cholesteric LC microdroplets [17]. Kumar *et al.* showed that WGM resonance can be a diagnostic tool for detecting subtle phase transition in liquid crystals [18]. Thermal applications based on the WGMs of cholesteric LC microdroplets have been reported by Wang *et al.* [19]. Very recently we have shown the effect of a magnetic field on the structure and WGM lasing of ferromagnetic nematic LC microdroplets [20]. In this paper, we report experimental studies on the effect of the temperature and electric field on the quality factor and free spectral range (FSR). We show that the variation of these two resonance properties can be understood based on the effective refractive index of the microdroplets observed by the circulating light. Their high sensitivity and easy tunability make them potential candidates for various applications in photonic devices.

II. EXPERIMENTAL

We used 4′-pentyl-4-biphenyl-carbonitrile (5CB) liquid crystal obtained from Sigma-Aldrich. It exhibits the following phase transitions: Cr 23.65°C N 33.5°C I. It shows positive dielectric anisotropy and positive birefringence. The LC microdroplets were suspended in polydimethylsiloxane (PDMS) using a micropipette. Prior to droplet formation a small quantity (2 wt%) of fluorescent dye [4-dicyanomethylene-2-methyl-6-(*p*-dimethylaminostyryl)-4H-pyran], commonly known as DCM, was doped. The LC-polymer mixture is confined between two indium-tin-oxide coated glass plates. Microdroplets of the desired size were excited with a focused laser light of wavelength 532 nm (Nd:YAG second harmonic). The absorption peak of the DCM dye coincides with the wavelength of the laser light. The resonance spectra coming from the microdroplets were studied with the help of a scanning near-field optical microscope (WiTec Alpha-200) fitted with a spectrometer. The minimum spectral resolution of the spectrometer is 0.09 nm. A schematic of the experimental setup is shown in Fig. 1. To study the effect of an electric field a sinusoidal voltage was applied across the cell with the help of a function generator (Tektronix-AFG 3102) and a voltage amplifier (TEGAM-2350). A temperature controller (Instec Inc. mk1000) was used to vary the sample temperature.

III. RESULTS AND DISCUSSION

A polarized optical micrograph of PDMS film with 5CB liquid crystal droplets is shown in Fig 2. A large number of spherical droplets of various sizes are formed. Figure 3(a) shows an isolated microdroplet under a polarizing optical microscope. Colorful rings appear due to the varying optical retardation from the center to the periphery. Four extinction branches originating from the center of each droplet are oriented along the polarizer axes. This suggests that the director is radially symmetric and the long molecular axes are orthogonal to the liquid crystal–PDMS interface. Figure 3(b) shows a schematic of the director orientation in a microdroplet with a radial hedgehog defect at the center. We focused on an isolated microdroplet and excited it with laser light (532 nm) just inside the polymer–liquid crystal interface as the resonant modes are formed inside. The irradiation point is indicated by the arrow in Fig. 3(c). The dye molecules emit

*sdsp@uohyd.ernet.in

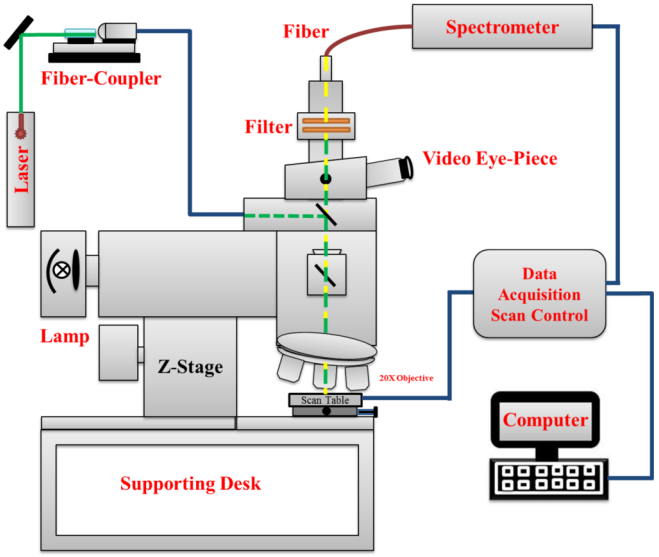

FIG. 1. Schematic of the scanning near-field optical microscope setup.

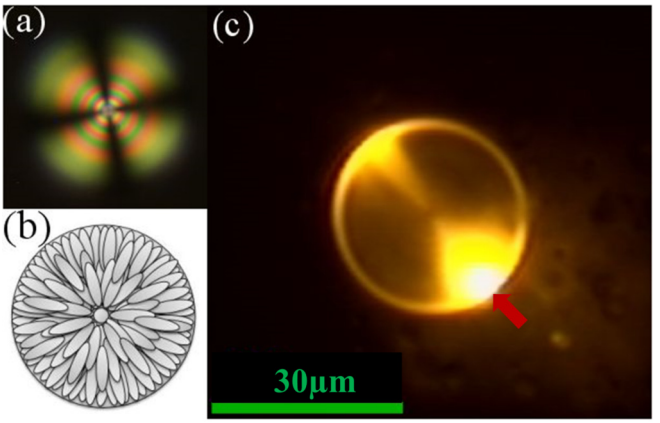

FIG. 3. (a) Polarizing optical micrograph of a focused 5CB microdroplet. (b) Schematic showing the molecular orientation inside the microdroplet. (c) A DCM dye–doped micro-droplet illuminated with a focused laser beam ($\lambda = 532$ nm). The red arrow indicates the irradiation point.

fluorescence and a thin light ring around the circumference of the microdroplet is observed, indicating the excitation of WGM resonance. The restricted fluorescence within the microdroplet suggests that the dye molecules are not diffused across the interface. The light emitted from the microdroplet is collected by the same objective and sent to the spectrometer. Figure 4(a) shows the characteristic resonance spectra obtained from a microdroplet at two temperatures. It is shown that the peak intensity of the modes decreases and the full-width at half-maximum increases with the temperature. The separation between any two consecutive modes is also increased at higher temperatures. Liquid crystals, being birefringent, possess different refractive indexes (ordinary and extraordinary) for different polarizations of light. The optic axis is radial, as the droplets exhibit a radial director structure. Hence the TE mode senses the ordinary (n_o) and the TM mode senses the extraordinary (n_e) refractive index. For 5CB, $n_e > n_o$ and they

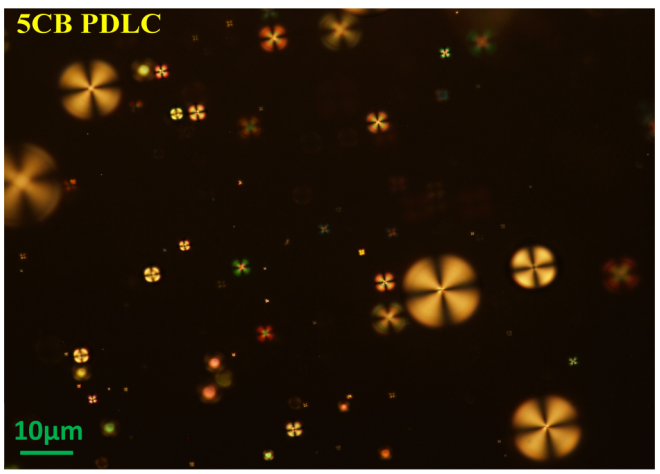

FIG. 2. Polarizing optical micrograph showing suspended micro-droplets of 5CB liquid crystal in PDMS at room temperature.

show opposite temperature dependences, i.e., n_e decreases, whereas n_o increases, as the temperature is increased towards the isotropic-nematic phase transition. On the other hand, the refractive index of PDMS remains constant ($n_s = 1.43$). For a smaller droplet size (diameter, $<15\mu$m) it can be shown that only TM modes with radial mode number $q = 1$ are supported [15,21].

To characterize the resonance spectra quantitatively, we measured the Q factor as a function of the temperature from the resonance line width of the mode with the highest intensity. It is given by $Q = \lambda/\Delta\lambda$, where $\Delta\lambda$ is the resonance line width corresponding to the resonant wavelength λ. Figure 4(b) shows the variation of the Q factor as a function of the temperature. The Q factor at room temperature is large (1150) and decreases rapidly as the temperature is increased towards the nematic-isotropic phase transition. For a spherical microresonator, the Q factor can be expressed as [14,22] $1/Q_{\text{tot}} = 1/Q_{\text{mat}} + 1/Q_{\text{rad}} + 1/Q_{\text{LC}} + 1/Q_{\text{ss}} + 1/Q_{\text{coupling}}$, where Q_{mat} refers to the intrinsic material loss due to absorption and scattering in the dielectric medium of the resonator. It is given by $Q_{\text{mat}} = 2\pi n_r/\lambda\alpha_{\text{mat}}$, where α_{mat} is the absorption decay constant and n_r is the refractive index of the resonator. The radiation loss Q_{rad} is due to the curvature of the microcavity. Q_{ss} refers to the surface scattering loss due to roughness, Q_{LC} refers to the loss due to the thermal fluctuations of the director, and Q_{coupling} refers to the losses involved in coupling into the external devices. The contribution of the intrinsic material loss Q_{mat} is directly proportional to the refractive index of the resonator and hence strongly depends on the temperature. The loss (Q_{LC}) due to the thermal fluctuations of the director is also expected to increase slightly with increasing temperature. Since the size of the droplet is very small and it supports only TM modes corresponding to the radial mode number $q = 1$, we can consider $n_r \simeq n_e$. The temperature dependence of n_e is given by $n_e = A_e - B_eT - C_e(1 - T/T_c)^{\beta}$, where A_e, B_e, C_e, and β are constants and T_c is the isotropic-nematic phase transition temperature. The exponent β is about 0.2 for 5CB [23]. Assuming that the major contribution to the temperature

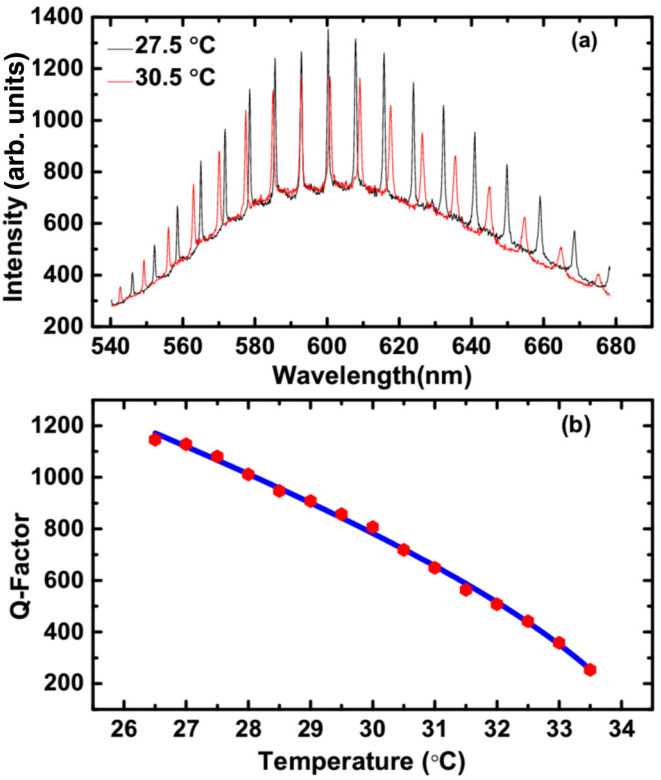

FIG. 4. (a) Representative WGM spectra recorded at two temperatures, namely, at 27.5°C (black line) and 30.5°C (red line). (b) Variation of Q factor with temperature. The solid line is the best fit to Eq. (1). Droplet diameter: 9 μm.

variation of Q comes from Q_{mat}, we can write

$$Q \approx A - BT - C\left(1 - \frac{T}{T_c}\right)^{\beta}. \tag{1}$$

The fitting of the Q factor with the temperature is shown in Fig. 4(b). The fit parameters obtained from the best fit are $A = 19\,776$, $B = 67$, $C = 3129$, and $\beta = 0.2$. Interestingly, this exponent (β) is comparable to the exponent of the temperature dependence of the extraordinary refractive index of 5CB [23]. It further confirms that the major contribution to the temperature dependence of Q comes from the change in the extraordinary refractive index. We also note that a very small change in the extraordinary refractive index can give rise to a substantial change in the Q factor (e.g., $\Delta n_e/\Delta Q \sim 3 \times 10^{-5}$ at room temperature).

We further studied the effect of an ac electric field on the Q factor of the optical resonance. The electric field creates elastic distortion of the director in the microdroplets beyond a particular value [14,24–26]. The typical distortions of the director under normal boundary conditions at zero, low, and high electric fields are shown schematically in Fig. 5. The change in the internal structure is expected to impact the resonance properties. We kept the temperature fixed in the nematic phase and collected the spectra at various voltages, and the Q factor was estimated from the line width of the mode with the highest intensity. Figure 6(a) shows typical spectra obtained at two voltages. Figure 6(b) shows the variation of the Q factor with the applied voltage. The Q

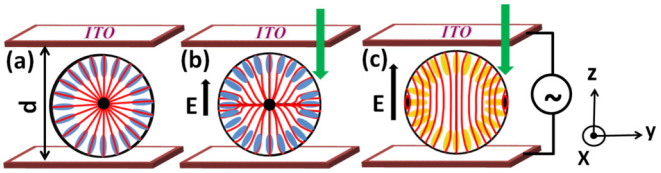

FIG. 5. Schematic showing the director field and resonance modes in a microdroplet at (a) zero, (b) small, and (c) large electric fields. Blue and yellow ellipsoids represent modes; red lines, the director. ITO, indium-tin-oxide.

factor remains unchanged up to a certain value and decreases rapidly with increasing voltage. The decrease in the Q factor can be understood based on the effective refractive index seen by the light due to the elastic distortion of the director. It is known that the LC director deforms inside the droplets beyond a particular voltage [14,25]. The effective refractive index of the nematic LC is given by [24]

$$n_{\text{eff}} = n_r = \sqrt{\frac{n_e^2 n_o^2}{n_o^2 \sin^2\theta + n_e^2 \cos^2\theta}}, \tag{2}$$

where θ is the angle between the propagation direction and the director (optic axis). This relation is usually appropriate for the uniform director field but this can be adapted to the present situation, especially near the equator where the modes are located (blue ellipsoids in Fig. 5). At zero field $\theta = 90°$ and $n_{\text{eff}} = n_r \simeq n_e$. In this case the director (near the equator

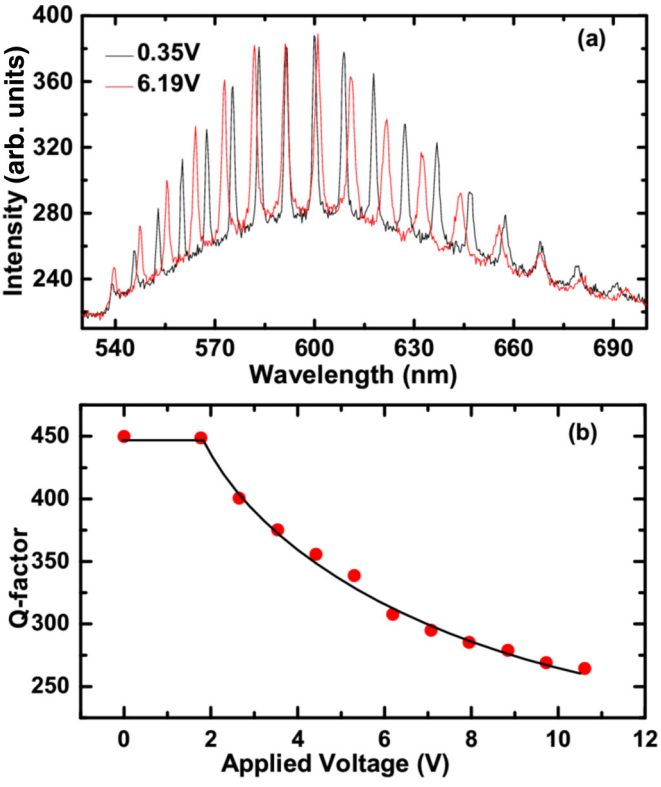

FIG. 6. (a) WGM resonance spectra at two voltages: 0.35 V (black line) and 6.19 V (red line). (b) Variation of the Q factor with the applied voltage. The solid line is a guide for the eye. Droplet diameter: 8 μm.

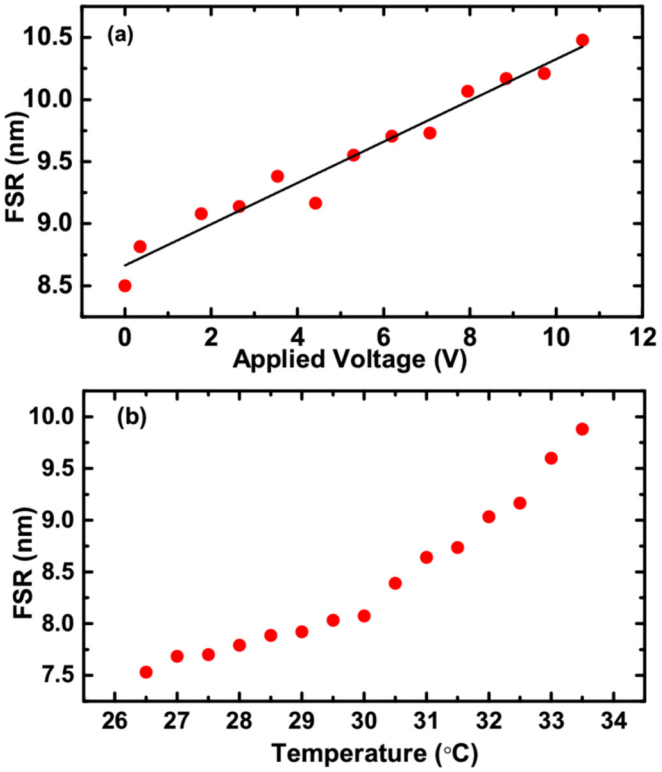

FIG. 7. (a) Variation of free spectral range (FSR) with applied voltage. The straight line is the best fit (linear) with a slope of 0.17 nm/V. (b) Variation of FSR with temperature.

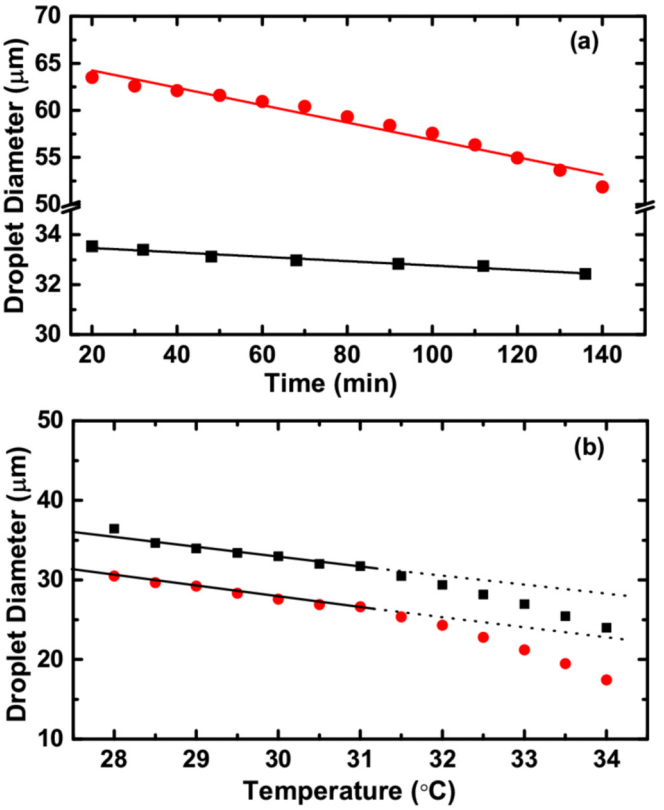

FIG. 8. (a) Variation of the diameters of microdroplets with respect to (a) time and (b) temperature. Lines in (a) are the linear best fits. The slope of the smaller droplet 33.5 (μm) is 9 nm/min. Dotted lines in (b) show the deviation from the linear variation.

of the droplets where the modes are located) tilts toward the direction of the electric field and n_{eff} ($\simeq n_r$) decreases. Since Q_{mat} is linearly proportional to n_r, it is expected to decrease with increasing field.

Careful observation shows [Fig. 4(a) and Fig. 6(a)] that the free spectral range, i.e., the separation of wavelengths between two consecutive modes ($\delta\lambda_{\text{SM}}$; denoted by the FSR) of the resonance also changes with increasing temperature and voltage. To quantify this we measured $\delta\lambda_{\text{SM}}$ as a function of the temperature and applied voltage and the results are presented in Fig. 7. It is shown that the FSR increases linearly with the applied voltage, and at the highest applied voltage (i.e., 11 V) the increment is about 2 nm [Fig. 7(a)]. Figure 7(b) shows the variation of the FSR with temperature. It also increases almost linearly with the temperature and changes slope at $\approx$31°C. The increase in FSR with increasing temperature and voltage can be expected due to the change in the effective refractive index of the microresonator assuming that the size remains unchanged. The FSR of a spherical microresonator is given by [1]

$$\text{FSR} = \delta\lambda_{\text{SM}} = \frac{\lambda^2}{2\pi n_r R}, \tag{3}$$

where R is the radius of the microresonator and λ is the resonant wavelength. When the temperature or the voltage is increased the effective refractive index (n_{eff}) decreases as discussed previously. Since n_{eff} ($=n_r$) is inversely proportional to the FSR, it is expected to increase in both cases.

A quantitative estimation of the FSR can be made from Eq. (3). For example, at $T = 26.5$°C and $T = 33.5$°C, the effective refractive indexes are given by $n_{\text{eff}} = 1.702$ and $n_{\text{eff}} = 1.672$, respectively [27]. The radius of the microdroplet is 4.5 μm and the resonant wavelengths at these two temperatures corresponding to the highest peaks are 603.3 nm and 602.3 nm, respectively [see Fig. 4(a)]. The calculated FSRs at these two temperatures are 7.5 nm and 7.65 nm, respectively. Thus the increase in FSR due to the increase in temperature (from 26.5°C to 33.5°C) is about 0.15 nm. But experimentally we find that the increase in FSR is about 2.3 nm [Fig. 7(b)]. Similarly, we estimate the FSR at zero and at the highest applied voltage. At zero voltage $\theta = 90°$, and from Eq. (1) we get $n_{\text{eff}} = n_e = 1.702$ [27]. Assuming that the director on the equator is completely reoriented along the field direction [i.e., $\theta = 0°$; see Fig. 5(c)] at the highest voltage we get $n_{\text{eff}} = n_o = 1.53$ [27]. The radius of the droplet is 4.0 μm and the resonant wavelengths are 604.3 nm and 598 nm, respectively [see Fig. 6(a)]. The estimated corresponding FSRs at the two voltages are 8.54 nm and 9.3 nm, respectively. Hence the maximum increase in the FSR due to the electric field is about 0.75 nm. But from the experiment we find that the FSR is increased by about 2 nm [Fig. 7(a)]. Therefore the experimentally observed enhancement of the FSR cannot be understood in either case from the decrease in the effective refractive index alone. This discrepancy motivated us to check the size of the droplets with time, as the FSR is inversely

proportional to the droplet radius (R). For this purpose we measured the diameters of a few microdroplets as a function of the time and temperature.

Figure 8(a) shows the variation of diameters of two different microdroplets with time. It is observed that the diameters of the microdroplets decrease with time and the rate is higher for larger microdroplets. For example, the initial diameter of a microdroplet with $D = 33.5\ \mu$m decreases to 32.5 μm over 140 min. Hence the radius ($R = D/2$) decreases at the rate of nearly 4.5 nm/min (from the slope). At the same rate a microdroplet of radius 4 μm [Fig. 6(a)] is expected to decrease to 3.42 μm during the experiment. Taking the reduced size into account (i.e., $R = 3.42\ \mu$m) and average refractive index $\overline{n} = 1.587$ [i.e., $(n_e + 2n_o)/3$], the estimated FSR from Eq. (3) is about 10.5 nm, which is similar to that shown in Fig. 7(a). Therefore the size reduction during the course of the experiment has a significant effect on the FSR. Figure 8(b) shows the variation of the diameters of two different microdroplets with the temperature. Initially the diameter decreases linearly with the temperature and beyond 31°C it decreases much more rapidly. The effect of the rapid size reduction beyond this temperature is reflected clearly in the temperature dependence of the FSR [Fig. 7(b)]. In particular, initially the FSR increases linearly with the temperature and at 31°C it changes slope and increases further.

IV. CONCLUSION

In conclusion, we have studied the effect of temperature and electric field on the quality factor and free spectral range of nematic liquid crystal microdroplets embedded in PDMS. The quality factor decreases significantly with increasing temperature due to the decrease in the extraordinary refractive index. With increasing electric field the quality factor also decreases beyond a particular voltage due to the decrease in the effective refractive index. The free spectral range increases with increasing temperature and voltage due to the reduction in the effective refractive index. Thus both the quality factor and the free spectral range can be tuned electrically and thermally. We find that the size reduction with time has a significant effect on the free spectral range. The experimental change in the free spectral range is in good agreement with the quantitative estimation based on the time-dependent size reduction of the microdroplets.

ACKNOWLEDGMENTS

We gratefully acknowledge the support from SERB (Grant No. EMR/2015/001566) and DST (Grant No. DST/SJF/PSA-02/2014-2015). J.A.S. acknowledges UGC for the BSR fellowship. We acknowledge the support of the Center for Nanotechnology, University of Hyderabad.

[1] K. Vahala, *Optical Microcavities* (World Scientific, Singapore, 2004).
[2] S. Arnold, S. Holler, and S. D. Druger, Optical processes in microcavities, in *Advanced Series in Applied Physics*, edited by R. K. Chang and A. J. Campillo (World Scientific, Singapore, 1996), Vol. 3.
[3] A. B. Matsko and V. S. Ilchenko, Quantum Electron. **12**, 3 (2006).
[4] A. B. Matsko and V. S. Ilchenko, Quantum Electron. **12**, 15 (2006).
[5] F. Vollmer and S. Arnold, Nat. Methods **5**, 591 (2008).
[6] S. Arnold, S. I. Shopova, and S. Holler, Opt. Express **18**, 281 (2010).
[7] X. Fan, I. M. White, S. I. Shopova, H. Zhu, J. D. Suter, and Y. Sun, Anal. Chim. Acta **620**, 8 (2008).
[8] S. Arnold, M. Khoshsima, I. Teraoka, S. Holler, and F. Vollmer, Opt. Lett. **28**, 272 (2003).
[9] F. Vollmer, S. Arnold, and D. Keng, Proc. Natl. Acad. Sci. USA **105**, 20701 (2008).
[10] M. Loncar, Nat. Photon. **1**, 565 (2007).
[11] H. Wang, L. Yuan, C.-W. Kim, Q. Han, T. Wei, X. Lan, and H. Xiao, Opt. Lett. **37**, 94 (2012).
[12] J. J. Yang, M. Huang, X. Z. Dai, M. Y. Huang, and Y. Liang, Europhys. Lett. **103**, 44001 (2013).
[13] L. He, S. K. Qzdemir, J. Zhu, W. Kim, and L. Yang, Nat. Nanotechnol. **6**, 428 (2011).
[14] M. Humar, M. Ravnik, S. Pajk, and I. Musevic, Nat. Photon. **3**, 595 (2009).
[15] M. Humar and I. Musevic, Opt. Express **18**, 26995 (2010).
[16] M. Humar and I. Musevic, Opt. Express **19**, 19836 (2011).
[17] Y. Wang, H. Li, L. Zhao, Y. Liu, S. Liu, and J. Yang, Appl. Phys. Lett. **109**, 231906 (2016).
[18] T. A. Kumar, M. A. Mohiddon, N. Dutta, N. K. Viswanathan, and S. Dhara, Appl. Phys. Lett. **106**, 051101 (2015).
[19] Y. Wang, H. Li, L. Zhao, Y. Liu, S. Liu, and J. Yang, Opt. Express **25**, 918 (2017).
[20] M. Marusa, J. A. Sofi, I. Kvasic, A. Mertelj, D. Lisjak, V. Niranjan, I. Musevic, and S. Dhara, Opt. Express **25**, 1073 (2017).
[21] C. C. Lam, P. T. Leung, and K. Young, J. Opt. Soc. Am. B **9**, 1585 (1992).
[22] M. L. Gorodetsky, A. A. Savchenkov, and V. S. Ilchenko, Opt. Lett. **21**, 453 (1996).
[23] J. Li, S. Gauza, and S. T. Wu, J. Appl. Phys. **96**, 19 (2004).
[24] L. C. Khoo, *Liquid Crystals* (Wiley-Interscience, Toronto, Canada, 2007).
[25] H. S. Kitzerow and P. P. Crooker, Liq. Cryst. **13**, 31 (1993).
[26] A. V. Koval Chuk, M. V. Kurik, O. D. Lavrentovich, and V. V. Sergan, Sov. Phys. JETP **67**, 1065 (1988).
[27] P. Karat, Ph.D. thesis, Raman Research Institute, Bangalore, India, 1977.